ELSEVIER

Journal of Alloys and Compounds 330–332 (2002) 8–13

Journal of ALLOYS AND COMPOUNDS

www.elsevier.com/locate/jallcom

Precepts and prospects for phase diagrams of M–H systems

F.D. Manchester*

Physics Department, University of Toronto, Toronto ON, M5S 1A7, Canada

Abstract

A collection totalling some 37 binary metal–hydrogen (M–H) phase diagrams, has been assembled in a recently published monograph, with 20 of these being covered in considerable detail. From insight gained in this exercise, a selection has been made of some features of particular phase diagrams, those of the Fe–H, Nb–H and V–H systems, which should be of interest for the planning of future experiments. This work has, of course, made use of traditional principles in the compilation of phase diagrams from experimental data but it has also benefited from an increased inventory of constraints which is now available for M–H systems. A summary of this enhanced capability is presented.

Keywords: Thermodynamic constraints; Phase diagrams; Fe–H; V–H; Nb–H

1. Possibilities for future research based on information from phase diagram assessments

Below, three examples are given, in which the assessment of phase diagram information [1] has pointed to situations for which the resolution of a particular problem presents a scientifically interesting challenge or addresses an important technological goal. In the interests of brevity, only two phase diagrams are included in this presentation, others referred to may be found in [1].

1.1. Fe–H system

Problems with hydrogen embrittlement of iron and of ferrous alloys have provided motivation for investigations of the solubility of H in iron for many years but this still remains a problem which is, in large part, unsolved. There is very little phase diagram information for the Fe–H system which is correlated over the hydrogen pressure ranges that have been investigated (up to the beginning of the GPa region) and there is considerable evidence that H is not significantly absorbed into equilibrium interstitial positions in the Fe lattice for pressures below ~3.5 GPa [2–4]. In recognition of this, the Fe–H phase diagram related material of Ref. [1], contains no references to explicit phases of an Fe–H alloy for pressures below the GPa region, these having been replaced by 'allotrope references' which refer to the temperature range appropriate to a particular allotrope of pure Fe. Because of the historical record of harm caused by subjecting ferrous material to the presence of H, we assume that the H enters the Fe somehow, at pressures which are quite modest but there is no clear account, as yet, of just how this occurs. From the survey in [1], it seems that experimental methods which focus on sampling the H absorption characteristics of lattice imperfections are the most likely means of solving this puzzle. A technique which might be taken much further than it has been in the past, is tritium radiography [5]. This appears to provide evidence for absorption of H at grain boundaries, whereas an absence of this contribution to H absorption (for the αFe region, at least) was claimed by da Silva and McLellan [6], using another technique. If there is conflicting evidence here, the matter should be resolved but, in any case, wider investigation of grain boundaries, dislocations etc. in Fe and their relation to H absorption should be made.

For the Fe–H system, the determination of the P–T diagram in the GPa region is a situation more concerned with phase diagram delineation, than the above. Some earlier work on this diagram is in need of revision and some progress with this has already been made [7,8] but more clarification is still needed. A reviewer should not make light of the fact that this is a task requiring considerable effort.

1.2. ($\alpha'+\beta$) Region of the Nb–H phase diagram

The boundaries of this mixed-phase region are shown in Fig. 1. There are two principal points of interest concerning the ($\alpha'+\beta$) phase field, both of them relating to H

E-mail address: fd.manchester@utoronto.ca (F.D. Manchester).

0925-8388/02/$ – see front matter
PII: S0925-8388(01)01579-1

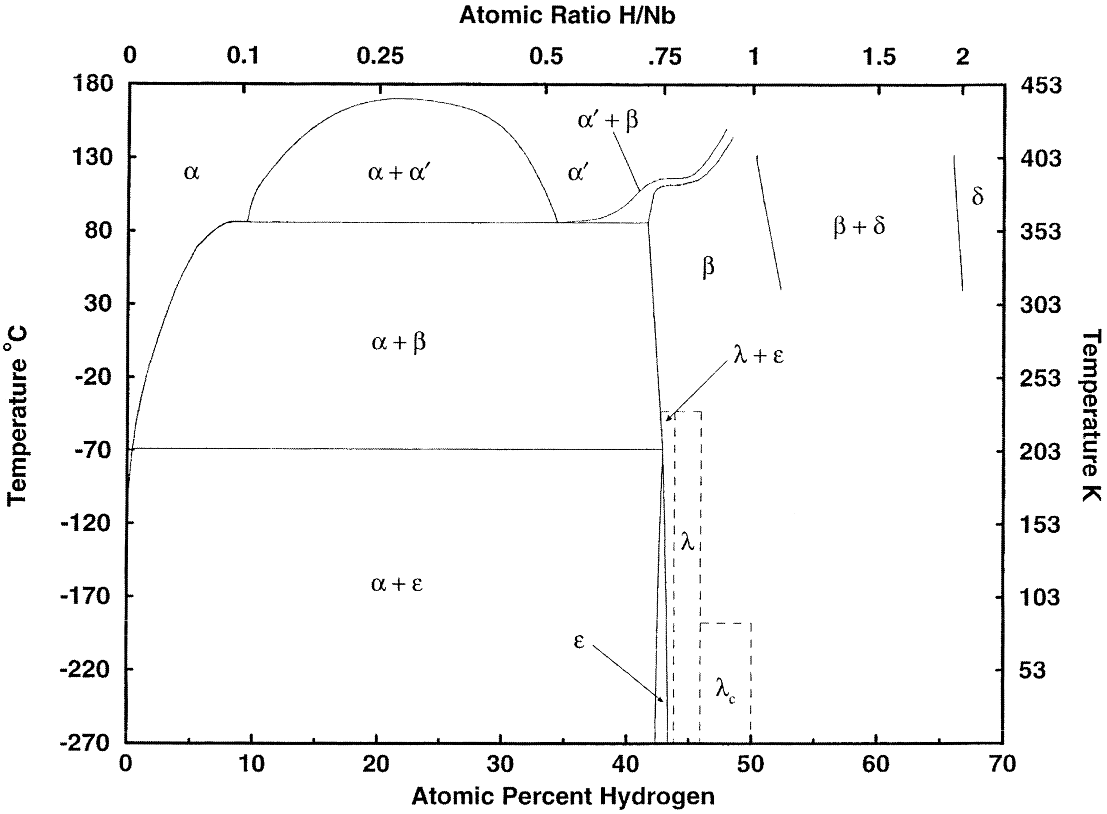

Fig. 1. Temperature–concentration diagram (incoherent) for the Nb–H system, after [1].

concentrations in the vicinity of $X=0.8$: one is that it has been reported [9,10] as having a temperature width of <1 K, and the other is that this phase field appears to have boundaries which are close to being horizontal (i.e. constant in temperature), in the region of $X\approx0.8$. The boundaries of the $(\alpha'+\beta)$ phase field drawn in Fig. 1, are an overall average of all the available data points and may not represent features from some individual measurements which have some significance not readily apparent in the averaging. To settle the matter of properly locating these boundaries requires a comprehensive set of measurements from one laboratory; the possibilities for superheating and other non-equilibrium effects should also be investigated. There is more involved here than just boundary location. The second of the points of interest, the horizontal phase boundaries, involves a concern with the Luo–Flanagan correlations (see below). One of these [Eq. (2)] relates the slope of a single-phase/two-phase boundary to the difference between the enthalpy of the single-phase and that of the two-phase region. With the slope of the $\alpha'/(\alpha'+\beta)$ boundary, for example, varying from ~1 to ~0 to ~1, in approximately the middle of its range, some questions are raised about enthalpy values along this boundary. For an M–H system with a miscibility gap [e.g. the $(\alpha+\alpha')$ mixed-phase region of Nb–H] the Luo–Flanagan correlations function well, away from the critical-point region. At the critical point, the slope of the boundary is zero and the critical point transition is not first-order. In fact, because one has to allow for the possibility of a transition in a coherent as well as an incoherent crystal, for temperatures just below the critical point, the transition at the boundary of the miscibility gap may not be first order for some distance on either side of the critical point, only becoming first-order for temperatures below the tri-critical points located symmetrically about the critical point, on a spinodal[1]. Viewed in terms of this picture, it would be interesting to have a determination of just how close to zero the boundary slopes for the $(\alpha'+\beta)$ mixed-phase region are, for $X\approx0.8$ and to have enough detailed information on the configuration of the boundaries to be able to understand what transitions might be involved in this region of the phase diagram.

1.3. β_1/β_2 Boundary of the V–H system

A number of independent investigations, summarized in [1], have identified the β_1/β_2 boundary as a line of second order (critical point) transitions and as such, it could be terminated, at its high temperature end, in a tricritical point [11,12]. A way in which this requirement could be accommodated was suggested by Moss [13] and this has been incorporated in Fig. 2. Moss and co-workers have

---

[1] See Fig. 3 of Part II of Nb–H assessment in Ref. [1].

have examined the $\beta_1 \leftrightarrow \beta_2$ transition, with an emphasis on obtaining critical point exponents which could establish the identification of a tricritical point termination for the β_1/β_2 boundary. Although a considerable amount of detailed information is available from these investigations, it is still not clear that the existence of a tricritical point termination for the upper end of this boundary has been established (see [1]). There should be more than one way of obtaining supporting evidence for the existence of such a tricritical point. An examination of the V–H phase boundaries in the vicinity of the suggested tricritical point, in Fig. 2, shows that the data giving the locations of these boundaries are rather sparse (see [1]). Improved delineation of these boundaries would help in determining if a tricritical point was present. Clear identification of a tricritical point at this location would be interesting for the physics of transitions generally, not just for the properties of M–H systems.

Currently available evidence [14] indicates that the β_1/β_2 boundary exists as a locus of second order transitions, down to 25°C and at $X \approx 0.7$ and the question naturally arises as to how this boundary is terminated in this part of the phase diagram. Fukai and Kazama [15] have suggested, on the basis of information available to them at the time, that the β_1/β_2 boundary tended to become obscured for H concentrations approaching $X \approx 0.65$, because of a gradual loss of distinction between the Oz_1 and Oz_2 sublattices (see [1]). Whatever microscopic mechanism may be acting in this region of the β_1/β_2 boundary, the question of its termination as a line of critical points remains. Thus the acquisition of more detailed information on the form of the β_1/β_2 boundary near both of its known extremities would seem to be a worthwhile task.

2. Use of constraints in constructing phase diagrams

In addition to the Gibbs phase rule and other well known constraints, there are some which have become available in recent years which have particular applicability to the phase diagrams of M–H systems. We present below, a brief description and discussion of such constraints.

2.1. Speiser eutectoid relation

From the early work of Ells and McQuillan [16] on the Zr–H system, Speiser [17] drew attention to the fact that the hydrogen pressure vs. temperature relations for the three mixed-phase ($\alpha+\beta$), ($\beta+\delta$) and ($\alpha+\delta$) regions, intersected at a single point and that consequently the three

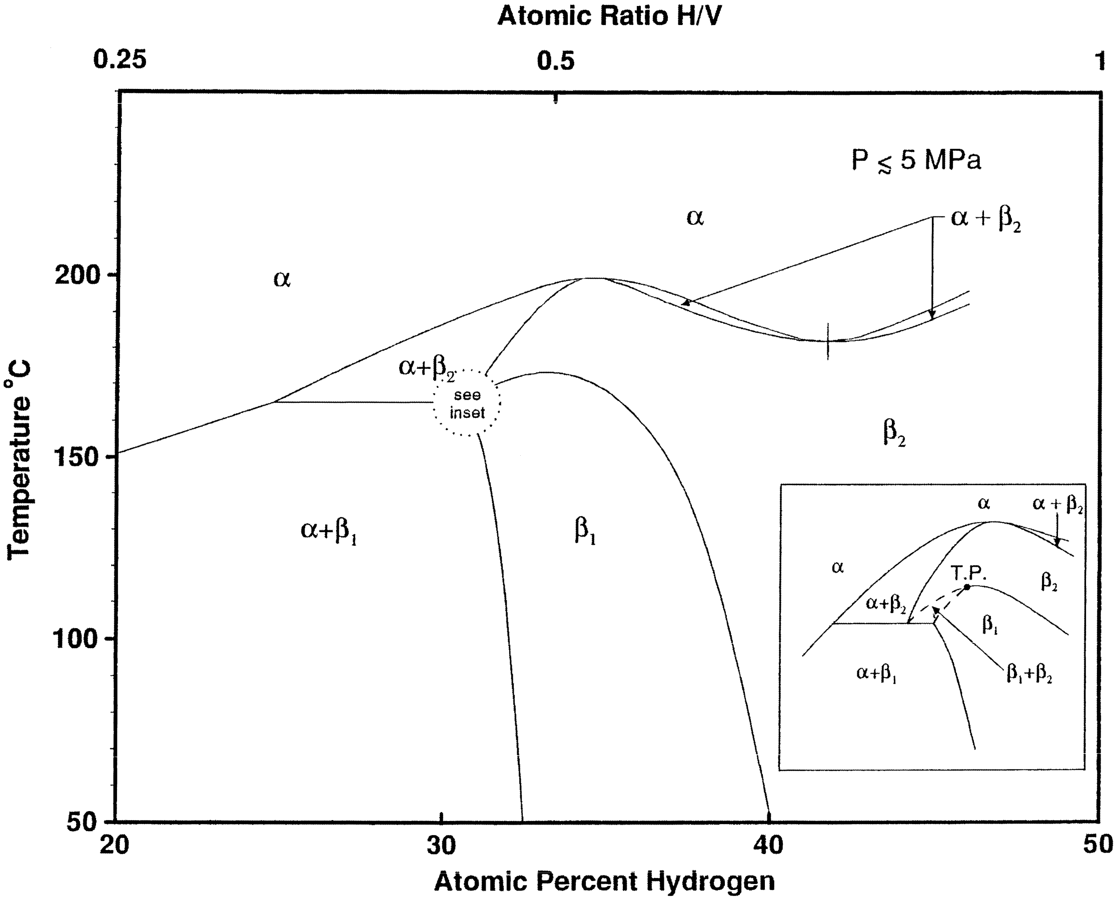

Fig. 2. Part of the temperature–concentration diagram for the V–H system, after [1].

two-phase equilibria are interrelated, so that the fugacities of H_2 for each univariant equilibrium may be written as

$$(X_\delta - X_\alpha)\frac{\mathrm{d}\ln f_{H_2}^{1/2}(\alpha,\delta)}{\mathrm{d}\,(1/T)} = (X_\beta - X_\alpha)\frac{\mathrm{d}\ln f_{H_2}^{1/2}(\alpha,\beta)}{\mathrm{d}\,(1/T)} + (X_\delta - X_\beta)\frac{\mathrm{d}\ln f_{H_2}^{1/2}(\delta,\beta)}{\mathrm{d}\,(1/T)}$$

where X_α, X_β and X_δ, are the intercepts of the respective single-phase regions with the eutectoid reaction isotherm. For the H_2 pressures involved, the fugacities in the above equation may be replaced by the hydrogen pressures with no significant error and this, in turn, leads to the relation

$$(X_\delta - X_\alpha)\,\Delta H_{\alpha,\delta} = (X_\beta - X_\alpha)\,\Delta H_{\alpha,\beta} + (X_\delta - X_\beta)\,\Delta H_{\delta,\beta} \tag{1}$$

between the enthalpies of the three mixed-phase regions.

The usefulness of this relationship may be illustrated by the example of determining X_δ, the high-concentration end point of the eutectoid reaction isotherm for the Ti–H system [1]. Earlier attempts [18] at locating a value for X_δ had been influenced by the trend of the P–T–X measurements of McQuillan [19], into making an extrapolation to a value of $X_\delta = 1.05$ (51.2 at.%H) but a revised attempt, making use of a very careful determination of the location of the eutectoid point by Bashkin et al. [20] together with the Speiser relation of Eq. (1), gave a value of $X_\delta = 1.40$ (58.3 at.%H) (see [1] for details). This value for X_δ suggests the presence of some error in the McQuillan [19] measurements but gives good agreement with other available P–X–T data for the $(\beta+\delta)/\delta$ boundary. Reliable calorimetric values for the enthalpies of the mixed-phase regions, such as the measurements of Dantzer and Luo et al. (see [1]) for the case of the Ti–H example cited here, have made the Speiser relation a constraint which is usefully quantitative in phase diagram compilations [1].

2.2. Luo–Flanagan coexistence boundary correlations

Luo and Flanagan [21] have listed a set of guidelines and correlations applicable to phase diagram behavior of metal–hydrogen systems. Of particular interest, in the present context, is the correlation involving changes in enthalpy that are measured as the boundaries between single-phase regions and two-phase regions of such a phase diagram are crossed, at constant temperature. Luo and Flanagan used a relationship from an earlier analysis [22], which expresses the difference between the enthalpy contribution of hydrogen in the two-phase region, $(\Delta H)^{\mathrm{II}}$ and that for the single-phase region, $(\Delta H)^{\mathrm{I}}$, in the form

$$(\Delta H)^{\mathrm{II}} = (\Delta H_{\mathrm{H}})^{\mathrm{I}}_{\mathrm{PB}} + \frac{R}{2}\left(\frac{\partial \ln P}{\partial X}\right)^{\mathrm{I}}_{T}\left(\frac{\mathrm{d}X_{\mathrm{PB}}}{\mathrm{d}(1/T)}\right) \tag{2}$$

where the subscript PB denotes the value of a quantity on the single-phase/two-phase (i.e. I/II) boundary, the superscripts I and II represent quantities evaluated for single and two-phase regions, respectively and P is the hydrogen pressure at a temperature T. As the concentration derivative of the hydrogen pressure is always positive in a single-phase region, the type of discontinuity encountered on crossing a I/II boundary, will depend on the sign and the magnitude of the slope for that boundary. For example: if a I/II boundary is vertical at temperature, T, then $\mathrm{d}X_{\mathrm{PB}}/\mathrm{d}(1/T) = 0$ and there is no difference between $(\Delta H)^{\mathrm{II}}$ and $(\Delta H)^{\mathrm{I}}$, as long as $(\partial \ln P/\partial X)^{\mathrm{I}}_{T} \neq \infty$. A good illustrative example of the value of Eq. (2) was originally given by Luo and Flanagan [21], a comparison between calorimetric measurements of the enthalpy made on the Ti–H and Zr–H systems. For the Ti–H system and a measuring temperature of 737 K, the $\alpha/(\alpha+\beta)$ boundary is crossed at a point where its slope is positive and therefore, according to Eq. (2), $(\Delta H)^{\mathrm{I}}$ should be less than $(\Delta H)^{\mathrm{II}}$, i.e. $|\Delta H|$ undergoes a step increase as the measurements proceed into the II region, a prediction confirmed by the measurements of Dantzer [23]. For the Zr–H system, which has a phase diagram very similar to that of Ti–H in the eutectoid region but without a retrograde form for the $\alpha/(\alpha+\beta)$ boundary, a measurement temperature of 928 K means that the $\alpha/(\alpha+\beta)$ boundary is crossed where its slope is negative and thus there should be a step down in the value of $|\Delta H|$ as the measurements proceed into the II region, a prediction borne out by the data of Dantzer et al. [25]. Thus the change in the slopes of the $\alpha/(\alpha+\beta)$ boundaries traversed during the two sets of measurements on these two systems, is consistent with the differences found between the enthalpy changes encountered in the calorimetry measurements, when these same two boundaries were crossed. This difference supports the retrograde form of the $\alpha/(\alpha+\beta)$ boundary for the Ti–H system, a support which is welcome, when the paucity of isotherm data available for the lower section of that boundary is considered.

2.3. α-Solvus condition

The relation expressing this condition, from [24,26], is

$$\Delta H_{(\mathrm{solvus})} = -\Delta H_{\alpha/\beta} + \Delta H^{\infty} \tag{3}$$

where $\Delta H_{(\mathrm{solvus})}$ is obtained from a fit to the solvus curve, the boundary between the α-phase and the α/β mixed-phase region, in this illustration; $\Delta H_{\alpha/\beta}$ is the plateau reaction enthalpy for the α/β mixed-phase region and ΔH^{∞} is the enthalpy at infinite dilution $(X \to 0)$ for the system.

Comparisons between values of $\Delta H_{(\mathrm{solvus})}$ calculated from Eq. (3) and those obtained from a fit to the solvus curve data are shown in Table 1. Except for the entries for the V–H system, the agreement between the experimental and calculated values for $\Delta H_{(\mathrm{solvus})}$ in Table 1 is fairly close. The enthalpy values used in Eq. (3) for the

Table 1

System	$\Delta H_{(\mathrm{solvus})}$ kJ/0.5 mol H_2 Expt.	$\Delta H_{(\mathrm{solvus})}$ kJ/0.5 mol H_2 Calc. (Eq. (3))	Ref.
Nb–H	11.2	11.2	[1]
Ti–H	22.9	22.2	[24]
V–H	13.6	10.1	[1]
Zr–H	36.7	37.7	[25]

comparison made for the V–H system, were obtained from calorimetry, so that it is unlikely that the enthalpy data were the cause of discrepancies shown for this system. Two conditions were given in [26] for Eq. (3) to give satisfactory agreement with the experimental value for $\Delta H_{(\mathrm{solvus})}$; for brevity we focus on just one of these, that the regular interstitial solution model applies to the M–H alloy under the conditions applicable in the consideration of its solvus. The regular solution model assumes that the H in the metal is so dilute that the mutual interaction among the H may be taken to be zero, an assumption that can be compared with experiment in the case of the Nb–H and V–H systems. The data of Schaumann et al. [27], taken at H concentrations comparable to those for which the solvus curves for Nb–H and V–H were determined, display Gorsky effect evidence for elastic interaction between the hydrogens in the Nb–H and V–H systems. Reference to the Gorsky effect evidence is not made to differentiate between measurements listed in Table 1 but to show that at least two of them were not made within the requirements of the regular solution model.

The form of Eq. (3) and the data assembled in Table 1, suggest that the α-solvus condition could be a useful check for relating thermodynamic data to phase diagrams but it seems that the terms of reference for establishing this relationship and, perhaps, the detailed form of the relation of Eq. (3), are in need of further examination.

2.4. Third law constraint

In a number of cases, e.g. [28,29], published (T–X) phase diagrams for M–H systems have shown fields of single phases tapering to zero breadth as the temperature nears absolute zero. In this type of presentation, the aim is to demonstrate that the entropy of mixing associated with the mixed-phase regions of the phase diagram, should tend to zero as the alloy system obeys the third law of thermodynamics in approaching the absolute zero. The third law requirement would be satisfied if the boundaries of the single-phase regions contracted in a manner that left no individual contribution from any of them as $T \rightarrow 0$. In contrast to other constraints for phase diagrams, this one invites more than one response. The alternative to tapering the boundaries, is to take the approach that the phase diagram presentation serves as an indication of what may be encountered when the particular system is experimentally investigated. In [1], the latter choice was made, for the reasons given below.

Even with one of the alloy constituents being highly mobile hydrogen, it will be increasingly difficult for the alloy phase boundaries to change their configuration as the alloy is cooled below room temperature; i.e. a significant entropy of mixing will remain ‘frozen in’ well before the alloy temperature nears absolute zero. A system which provides a singular exception to such a freezing-in process is the isotopic mixture of He^3 and He^4, which remains liquid under its vapor pressure for temperatures less than 1 K. For this system, sheding of the entropy of mixing occurs through phase separation in the liquid, so that a lighter He^3-rich portion ‘floats’ above a He^4-rich portion, with the degree of isotope separation increasing as the temperature is lowered (see [1]). In contrast, M–H alloys are solids at room temperature and below and hydrogen mobility, as it affects the movement of phase boundaries, becomes very much reduced below room temperature [1]. In view of these limitations, M–H alloy systems do not have mechanisms available for losing a significant fraction of their entropy of mixing with lowering temperature, let alone losing all of it, as implied by tapering of the boundaries for single-phase fields to zero width.

References

[1] F.D. Manchester (Ed.), Phase Diagrams of Binary Hydrogen Alloys, ASM International, Materials Park, OH, 2000.

[2] Y. Fukai, A. Fuzizawa, K. Watanabe, M. Amano, Jpn. J. Appl. Phys. 21 (1982) L318.

[3] J.V. Badding, R. J Hemley, H.K. Mao, Science 253 (1991) 421.

[4] I. Choe, R. Ingalls, J.M. Brown, Y. Sato-Sorenson, R. Mills, Phys. Rev. B 44 (1991) 1.

[5] M. Aucouturier, in: C.G. Interrante, G.M. Pressouyre (Eds.), Proceedings 1st Int. Conference on Current Solutions to Hydrogen Problems in Steels, American Society for Metals, Metals Park, OH, 1982, p. 407.

[6] J.R.G. da Silva, R.B. McLellan, J. Less-Common Metals 50 (1976) 1.

[7] M. Yamakata, T. Yagi, W. Utsumi, Y. Fukai, Proc. Jpn. Acad. B 68 (1992) 172.

[8] Y. Fukai, M. Yamakata, T. Yagi, Z. Phys. Chem. 179 (1993) 119.

[9] J.M. Welter, F. Schoendube, J. Phys. F, Met. Phys. 13 (1983) 529.

[10] D. Wlosewicz, T. Plackowski, N.I. Sorokina, Physica B 212 (1995) 113.

[11] R.B. Griffiths, Phys. Rev. Lett. 24 (1970) 715.

[12] I.D. Lawrie, S. Sarbach, in: C. Domb, J.L. Lebowitz (Eds.), Phase Transitions and Critical Phenomena, Vol. 9, Academic Press, London, 1984, p. 2.

[13] S.C. Moss, in: P. Jena, C.B. Satterthwaite (Eds.), Electronic Structure and Properties of Hydrogen in Metals, Plenum Press, New York, 1983, p. 153.

[14] W. Luo, J.D. Clewley, T.B. Flanagan, J. Chem. Phys. 93 (1990) 6710.

[15] Y. Fukai, S. Kazama, Acta Metall. 25 (1977) 59.

[16] C.E. Ells, A.D. McQuillan, J. Inst. Met. 85 (1956) 89.

[17] R. Speiser, in: W.M. Mueller, J.P. Blackledge, G.G. Libowitz (Eds.), Metal Hydrides, Academic Press, New York, 1968, Chapter 3.

[18] A. San-Martin, F.D. Manchester, Bull. Alloy Phase Diagrams 8 (1987) 30.

[19] A.D. McQuillan, Proc. Roy. Soc. (Lond.) A204 (1950) 309.

[20] I.O. Bashkin, A.F. Gurov, V.Y. Malyshev, E.G. Ponyatovsky, Sov. Phys. Solid State 34 (1992) 674.

[21] W. Luo, T.B. Flanagan, J. Phase Equilibria 15 (1994) 20.

[22] T.B. Flanagan, J.F. Lynch, J. Phys. Chem. 79 (1975) 444.

[23] P. Dantzer, J. Phys. Chem. Solids 44 (1983) 913.

[24] W. Luo, J.D. Clewley, T.B. Flanagan, Metall. Trans. B 24 (1993) 867.

[25] P. Dantzer, W. Luo, T.B. Flanagan, J.D. Clewley, Metall. Trans. A 24 (1993) 1471.

[26] T.B. Flanagan, W.A. Oates, S. Kishimoto, Acta Metall. 31 (1983) 199.

[27] G. Schaumann, J. Völkl, G. Alefeld, Phys. Stat. Sol. 42 (1970) 401.

[28] U. Köbler, J.M. Welter, J. Less-Common Met. 84 (1982) 225.

[29] T. Schober, in: Electronic structure and properties of hydrogen in metals, P. Jena, C.B. Satterthwaite (Eds.), NATO Conference Series VI: Materials Science, Vol. 6, 1983, p. 1.